JOURNAL OF CATALYSIS 146, 228–236 (1994)

Thermal Analysis of Adsorbed Propanamines for the Characterization of Ga–MFI Zeolites

Vladislav Kanazirev,[1] Kerry M. Dooley, and Geoffrey L. Price

Department of Chemical Engineering, Louisiana State University, Baton Rouge, Louisiana 70803

Received July 6, 1993; revised October 14, 1993

Gallium-containing forms of MFI zeolite have been subjected to adsorption of 1- and 2-propanamine, and the results of subsequent thermal treatment have been analyzed and compared to literature reports for propanamines adsorbed on proton forms of MFI. Zeolitic gallium cations show completely different behavior from zeolitic protons, including a propanamine decomposition mechanism which is different from Hofmann elimination. In this mechanism NH_3 is desorbed at temperatures as much as 160 K below that of H–MFI. Major differences in the decomposition chemistry of the two amines were also observed when Ga cations were present. © 1994 Academic Press, Inc.

INTRODUCTION

Zeolite-based catalysts are widely applied in a number of industrial processes including catalytic cracking, isomerization, and alkylation (1, 2). New processes using zeolites, e.g., methanol to hydrocarbons and aromatization of light paraffins, are still under investigation for large-scale operations (3, 4). It is well known that the efficiency of zeolites as catalysts is often determined by their acidic properties so that the study of the nature, number, and strength of the acid sites in zeolites continues to be of great importance in both basic and applied science.

The adsorption of thermally stable basic compounds such as ammonia and pyridine followed by temperature programmed desorption (TPD) is a widely used technique for the characterization of zeolite acidity (5–8). IR spectroscopy used in conjunction with pyridine adsorption can be used to distinguish between pyridine coordinated to Lewis acid sites and pyridinium ions associated with Brønsted acid sites (5–10). Virtually no thermal or catalytic decomposition of ammonia or pyridine has been observed during the TPD experiments.

Recently, Gorte and co-workers in a series of publications (11–19) have described a novel approach for the determination of the proton acidity of zeolites and related materials using thermal analysis (TA)[2] under vacuum conditions. They have been able to prove the formation of stoichiometric 1 : 1 complexes of simple organic molecules such as alcohols and amines with Brønsted acid sites. These complexes have been found to decompose during the course of TA yielding simultaneously an alkene and either ammonia (from amines) or water (from alcohols) (11–17). This mode of decomposition is well known in classic organic chemistry as Hofmann elimination, though the appropriateness of using this name for reactions of amines on solid surfaces has recently been questioned (20). Gorte and co-workers have shown the applicability of this approach for studying the proton acidity of a variety of catalysts including HZSM-5 (13, 14), isomorphously substituted ZSM-5 (15, 16), and aluminophosphates (18, 19). In the case of H–[Ga]–ZSM-5, they have found clearly defined adsorption complexes of 2-propanol and 2-propanamine with the protons associated with framework Ga. No such complexes have been observed with extra-framework Ga (15).

The work of Gorte and co-workers has proven that the Brønsted acidity of various zeolites and aluminophosphates can be measured using unstable basic compounds such as alkylamines as a probe. But for faujasites where the number of Brønsted acid sites may be less than the number of framework Al atoms, an accurate Al content cannot be obtained using this method (13). Similar complications have been reported for steamed materials probably due to structural changes which generate new types of acid sites (13). Although some work on materials that contain Lewis sites (e.g., alumina (21)) has been reported, the applicability of Gorte's method for the characterization of zeolite catalysts which contain both Brønsted and Lewis sites has, to our knowledge, never been reported.

---

[1] On leave from the Institute of Organic Chemistry, Bulgarian Academy of Sciences.

[2] Here, we use the term "thermal analysis" to mean the analysis of a process that occurs upon a linear temperature increase. The process could be desorption, decomposition, or any other reaction while the detection system is virtually unlimited. In this paper, we utilize a mass spectrometer and microbalance.

0021-9517/94 $6.00

In a very recent paper (22), 2-propanamine adsorption and subsequent TA on Cu^{2+} containing HZSM-5 has been reported. Upon Cu addition, a decline in Brønsted acidity and a new TA band at 650–800 K, thought to be due to Cu zeolitic cations, was detected.

In the present investigation, we used Gorte's method to study the acidity changes in HZSM-5 possibly occurring after its modification with gallium. While the parent zeolite has shown the expected TA features for both 1-propanamine (1-PA) and 2-propanamine (2-PA), the gallium-containing samples revealed a much different behavior. In this paper we show that Lewis acid sites such as nonprotonic zeolitic cations can give rise to another mode of propanamine adsorption and subsequent reaction upon temperature programming that deviates from the known Hofmann elimination route.

EXPERIMENTAL

UOP MFI zeolite with SiO_2/Al_2O_3 mole ratio of 40 was used as the catalyst base material in a fully protonated form which we refer to as H–MFI. A gallium-containing sample, designated Ga–MFI, was prepared by incipient wetness impregnation. Forty-two g H–MFI (10% water by weight) and 12 g $Ga(NO_3)_3 \cdot (H_2O)_8$ dissolved in 40 cm^3 deionized water were thoroughly homogenized and then dried in air at 383 K for 24 h. The catalyst was subsequently calcined in a tubular furnace purged with 3 vol% O_2 in argon at a total flow of 250 cm^3/min. The temperature was programmed from ambient to 393 K at 10 K/min, held at 393 K for 2 h, raised from 393 to 673 K at 2 K/min, and then held at 673 K for 6 h. Our previous investigations have shown (23) that a complete decomposition of the nitrate anion occurs using this calcination procedure. The Ga loading is equivalent to 7.1 g Ga_2O_3/100 g dry zeolite, which is about 0.95 Ga atoms/framework Al atom.

All catalysts under investigation were equilibrated in ambient air at room temperature, then pelletized and crushed to 0.18–0.42-mm-size particles prior to utilization.

A Perkin–Elmer TGA7 microbalance was used to detect weight change upon thermal treatment of the catalysts in He or a mixture of He with a reagent gas. Ten to 15 mg of sample was weighed out in the platinum microbalance pan. The following sequence of treatments was typically performed:

1. Drying in He flow (100 cm^3/min total) via temperature programming from 298 to 848 K at 10 K/min with a final hold of 10 min or more, followed by rapid cooling just prior to amine adsorption.

2. Propanamine adsorption for 5 min at 323 K. Propanamine was delivered to the microbalance sample by bubbling 50 cm^3/min of reagent gas (typically pure He) through the liquid at ambient temperature followed by further dilution with 50 cm^3/min pure He which purged the balance mechanism. The propanamine supply was then bypassed and the sample purged with pure He at 323 K for 10 min.

3. Thermal gravimetric analysis (TGA) in pure He by linear temperature programming from 323 to 823 K at 5 K/min.

In some cases, the amine adsorption was preceded by treatment of the catalyst with H_2 at 848 K using 75 cm^3/min He mixed with 25 cm^3/min H_2. The basis for assignment of 100% weight was taken as the dry weight before any treatment with propanamine. For propanamine adsorbates, a 1% weight change corresponds to 169.5 μmol/g zeolite.

TA with product detection by mass spectrometry (MS) was performed on an apparatus which has been described in detail previously (24). Briefly, 50 mg of catalyst was placed in a coaxial quartz tubular reactor (12 mm-o.d. jacket and 4 mm-o.d. inner tube) between a quartz frit and a plug of quartz wool. A thermocouple inserted into a coaxial reactor thermowell was used for temperature measurements. All thermal treatments of the catalyst samples were performed in the same manner as in the microbalance experiments including using a 100 cm^3/min flow rate of carrier gas, but a slightly different procedure for propanamine adsorption was applied. After drying in flowing He, the sample was cooled to 323 K and evacuated briefly, and then 0.2 bar propanamine was admitted and allowed to adsorb for 10 min. The catalyst was then evacuated for 10 min. and He flow was restored to purge the reactor. Finally TA was conducted in the same manner as in the microbalance experiments.

The reactor effluent was analyzed using a UTI 100C MS operated in EI mode at 70 eV. A jet separator roughed with an independent mechanical vacuum pump provided the interface to the reactor system. A cross-pattern leak valve was used to introduce about 20 cm^3/min of the reactor effluent into the mass spectrometer via the jet separator. A number of masses were continuously monitored during TA.

RESULTS

H–MFI Sample

The weight-versus-temperature (TA) and corresponding derivative (DTA) curves obtained in TA of 1-propanamine (1-PA) are depicted in Fig. 1. In accordance with the data of Gricus Kofke *et al.* (13) for HZSM-5 zeolites, a characteristic plateau appears in the TA curve in the temperature range 550–640 K. Following Gorte's interpretation (11–19) we assume that this plateau is due to the formation of a stoichiometric 1 : 1 complex of propanamine with zeolitic protons. Indeed, using the number

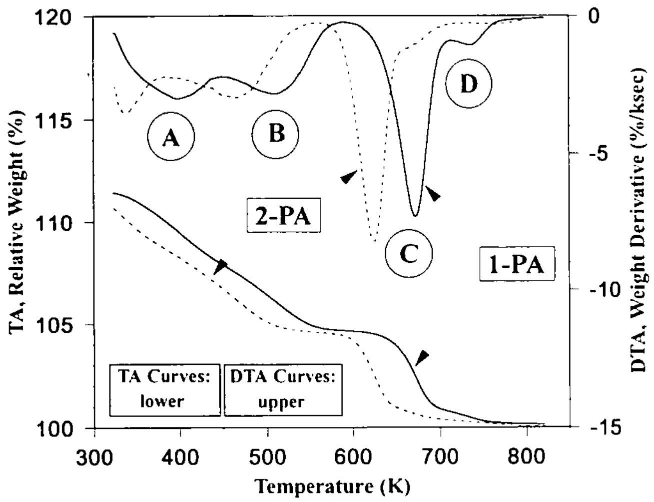

FIG. 1. Thermal analysis curves using microbalance (lower, TA; upper, DTA) for propanamines on H–MFI.

of 1-PA molecules adsorbed at the plateau in Fig. 1 and the aluminum content reported by the manufacturer of the H–MFI sample, we determine a ratio of 1.04. Moreover, the major peak C on the DTA curve for 1-PA shown in Fig. 1 is centered at 672 K, very close to the literature value of about 670 K for decomposition on HZSM-5 (Si/Al = 35) (17).

The TA–DTA curves for 2-propanamine (2-PA) shown in Fig. 1 provide further evidence for the formation of the 1 : 1 complex since the plateau is again present (0.99 2-PA molecules for each Al) while the major DTA peak is shifted 48 K lower compared to 1-PA. This shift is likely due to the higher reactivity of the isopropyl carbenium ion in the decomposition of the propanamine complex (13, 17). Both 1-PA and 2-PA as well as their desorption products are removed completely during the course of the experiment. The final weight of the sample deviates negligibly (about 0.1%) from the weight prior to propanamine adsorption.

Developing their method for Brønsted acidity measurement, Gorte and co-workers took special precautions to avoid bed effects in the desorption process. They (11–19) used low coverages of amine and small sample sizes (12–17 mg) spread flat on the sample pan in a microbalance mounted within a high-vacuum chamber. In our investigation, we applied more conventional equipment for the TA experiments. However, the size of the sample under study was kept small (10–15 mg) and a high He flow (100 cm^3/min) was used. The coverage of the catalyst with propanamine prior to TA was also substantially higher than in Gorte's work because we purged with pure He for only 10 min at 323 K. Despite altering Gorte's original procedure, we observe similar TA and DTA features. This suggests that any possible bed effects in the desorption process would be similar in both cases.

However, using the MS detector in a TA experiment, we note some differences between our results and Gorte's (13), which probably should be attributed to re-adsorption under the conditions employed in these experiments. In particular, we used more sample (50 mg) and therefore the bed was deeper. Furthermore, a stainless steel transfer line conveys the sample to the MS, and this may have contributed to chromatographic broadening, particularly for NH_3 which often interacts with active sites on stainless tubing. In Fig. 2, the TA curves for 1-PA show that an m/e = 17 (NH_3) band at 677 K appears slightly after an m/e = 41 band (propene) at 661 K, but in previous reports (13) these bands appear virtually simultaneously. TA of 2-PA (Fig. 2) shows even greater relative shifts in the positions of the mass spectral bands, particularly in that the m/e = 17 band is broadened and shifted to higher temperatures with respect to m/e = 41. Work reported by Gorte and co-workers (13) again shows nearly simultaneous elution of m/e = 17 and 41 except that a slightly higher temperature for m/e = 17 is visible. Note that smaller peaks for m/e = 41 at $T < 550$ K are the result of propanamine fragmentation, not propene desorption. This is important in the interpretation of all subsequent mass spectral data.

Beyond the problems already detailed, the results depicted in Figs. 1 and 2 clearly show other differences from the published data, namely the appearance of two additional bands designated A and D in Fig. 1. Peak A is clearly due to very weakly bound 1-PA and, in fact, previous investigators (13) were apparently able to remove this

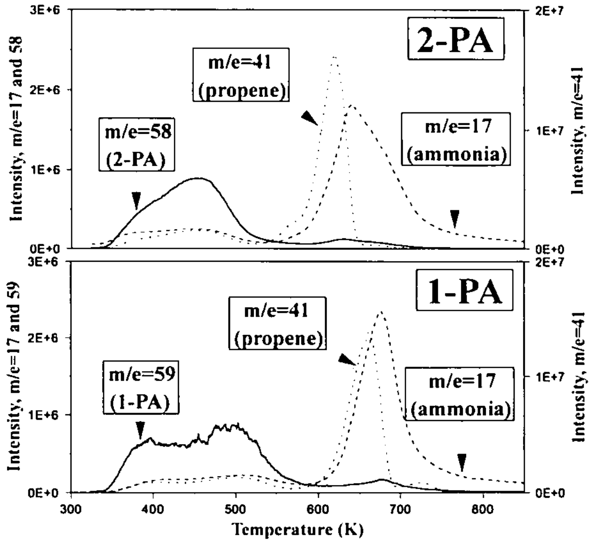

FIG. 2. Mass spectral analysis of the reactor effluent during thermal analysis of propanamines on H–MFI.

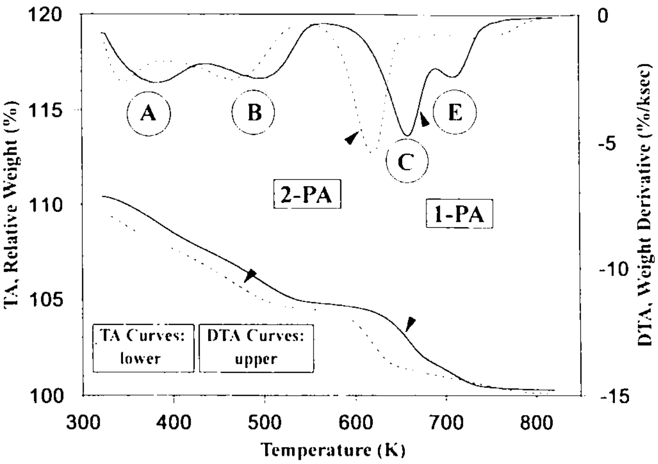

FIG. 3. Thermal analysis curves using microbalance (lower, TA; upper, DTA) for propanamines on unreduced Ga–MFI.

adsorbed species with extended evacuation. Interestingly, in both our and previous studies, it was observed that close to two 1-PA molecules/framework Al remain after desorption of peak A, either by temperature programming in our case or by extended evacuation as in previous studies (13). This suggests that a stoichiometric 2:1 1-PA:Al complex exists in the 400–450 K region. Physisorbed 1-PA exists in excess of the 2:1 complex below about 400 K. Thus, Peak B (Fig. 1) corresponds to the breakdown of the 2:1 complex which yields the 1:1 complex.

While Peaks B and C are in accordance with previous work, the existence of a high-temperature peak (denoted D in Fig. 1) has never been mentioned in the literature. This peak accounts for about 15% of the total adsorbed amount remaining in the "plateau" region. A careful examination of the mass spectral data from propanamine TA (Fig. 2) discloses that there is very little parallelism in the features of *m/e* = 41 (propene) band and *m/e* = 17 (ammonia) band in the temperature range 700–780 K, which suggests that propene and NH_3 evolution are at least partially decoupled in this region, rather than the direct coupling characteristic of Hofmann elimination in Peak C. Taking into account the rather high temperature of the sample pretreatment (843 K) used in our investigation, some Lewis acid sites should be present in the sample (25, 26). The interaction of the propanamine molecule with such tricoordinated and highly electron deficient sites might be the reason for the appearance of peak D.

Ga–MFI Sample

The TA and DTA curves of propanamines from the unreduced Ga–MFI sample are plotted in Fig. 3 and there are some desorption features similar to the unmodified H–MFI sample. Both propanamines show DTA peaks similar to the counterpart peaks originating from the unmodified sample and the major 2-PA peak is again shifted to a lower temperature compared to its 1-PA counterpart. The "plateau" region is still present in the TA curves for both propanamines, and 1.02 (1-PA) and 0.92 (2-PA) molecules/framework Al were still adsorbed in this region. Thus, if we had recorded only the sample weight and limited the final desorption temperature to the "plateau" region on the TA curves, we might have concluded that the introduction of Ga does not lead to changes in the Brønsted acidity. In fact, there are major changes in the DTA curves, especially for 1-PA desorption, consisting of:

(a) either the appearance of a new peak E in the DTA curve for 1-PA or a loss of resolution due to an increase in the intensity of the DTA peak D characteristic of H–MFI. Peak E is also noticeable for 2-PA desorption;

(b) a 40% reduction in the DTA peak C, ascribed in the case of H-MFI to the decomposition of the propylammonium cation (Brønsted acidity);

(c) a weight offset which is stable even after prolonged heating at 843 K. The residue accounts for about 5% of the propanamine adsorbed in the "plateau" region of the TA curves.

TA experiments with MS analysis of the reactor effluent confirmed the main phenomena observed for Ga–MFI in the microbalance. Figure 4 shows clearly the desorption of unreacted propanamine as indicated by *m/e* = 59 (for 1-PA) and *m/e* = 58 (for 2-PA) in the low-temperature range (323–523 K), similar to what was observed for H-MFI (Fig. 2). The MS data, however, confirmed that there

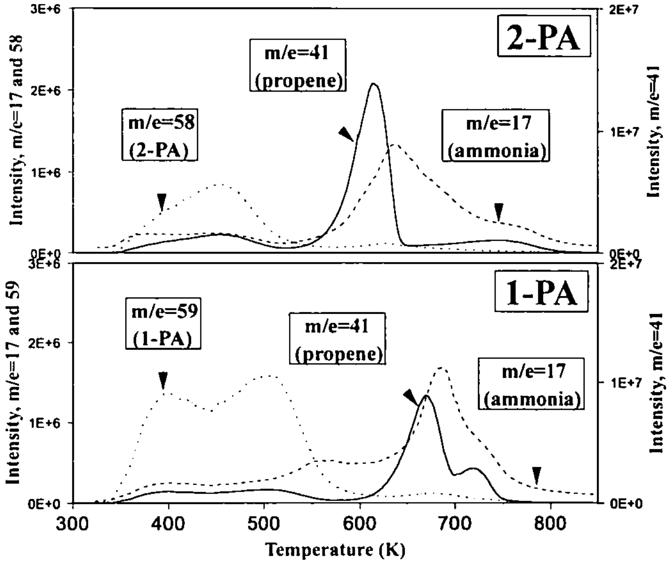

FIG. 4. Mass spectral analysis of the reactor effluent during thermal analysis of unreduced Ga–MFI.

are at least two significant changes in the desorption process due to the introduction of Ga into the H–MFI catalyst:

(d) A second high-temperature desorption peak for propene (m/e = 41) is clearly distinguished from the main desorption peak in the 1-PA spectra. However, this peak is apparently associated with peak E in the microbalance DTA curves. The ammonia content of the reactor effluent continuously decreases, although a shoulder is perhaps visible.

(e) Unexpectedly, the ammonia (m/e = 17) begins to desorb around 550 K at only a slightly higher temperature than the unreacted 1-PA. No such effect is detected in the case of 2-PA desorption.

As we have already mentioned, the desorption features obtained in the flow reactor might to some extent be affected by readsorption. Careful examination of the results, however, reveals that re-adsorption cannot be responsible for these two specific changes in the desorption–decomposition features of adsorbed propanamines, for the following reasons. First, the conditions of the microbalance experiment (small sample in flat pan) are more favorable for rapid removal of desorbed species than the conditions in the flow reactor. Despite this fact, an almost identical position of the desorption bands was observed in both cases. Second, if differences in readsorption behavior were responsible for new features (d) and (e) above, it would not be possible to explain the great disparities observed in these two new features when two similar compounds, 1-PA and 2-PA, desorbed from the same sample. With both compounds the maximum and plateau surface coverages were similar, and there was a common plateau temperature range. The origin of the disparities in features (d) and (e) must instead result from surface chemistry differences in the carbenium ion complexes which are formed during the decomposition reactions. The nature of these differences is further explored in the Discussion section.

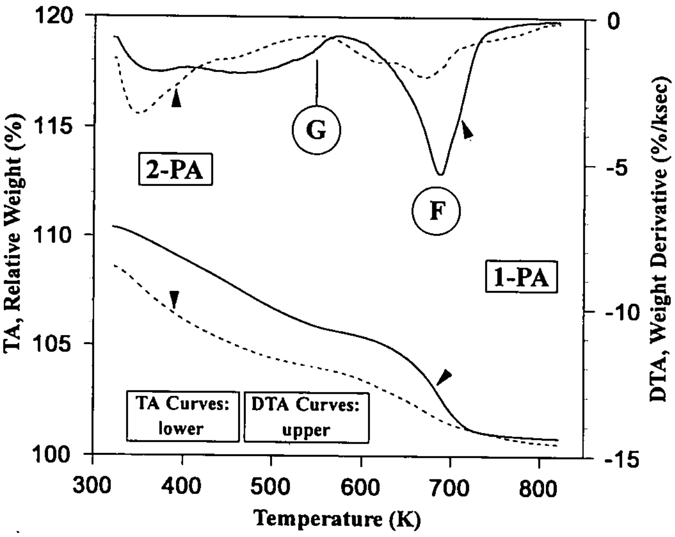

FIG. 5. Thermal analysis curves using microbalance (lower, TA; upper, DTA) for propanamines on reduced Ga–MFI.

The presence of Ga in the zeolite sample must be responsible for the appearance of new desorption features (d) and (e) discussed above. The impregnation procedure used for preparation of the Ga–MFI sample leads to formation of Ga_2O_3 well dispersed onto the microcrystallites of the H–MFI zeolite (27). Separate experiments have shown that pure Ga_2O_3 does not adsorb propanamines in any appreciable amount, and therefore a separate gallium oxide phase cannot be responsible for the specific changes (d) and (e) observed for TA of propanamines. The proton acidity of the catalyst has apparently changed after the introduction of Ga, as evidenced by a 40% decrease in intensity of the major peak C for both amines in the DTA curves for Ga-MFI (Fig. 3) compared to H–MFI (Fig. 1). However, the total (323 K) adsorption capacity for the propanamines did not change. The only reasonable explanation for these results is that some of the gallium nitrate used for impregnation has been ion-exchanged, such that some Ga ions have been incorporated into zeolitic cation positions. These electron-deficient species are apparently involved in a different mode or modes of interaction with propanamines.

Recently, in a series of publications (23, 28–32) we have reported that reduction of impregnated or mechanically mixed Ga_2O_3/HZSM-5 catalysts with H_2 or hydrocarbons is an effective method for incorporation of Ga^+ into the cationic positions of the zeolite framework. In the present investigation we have also used H_2 reduction of Ga–MFI to replace protons in the parent H–MFI with Ga^+ ions. New microbalance TA experiments have provided additional evidence for ion exchange during the preparation of the Ga–MFI sample. The observed weight decline upon H_2 reduction of Ga–MFI at 843 K for 3 h was 1.15%, which is less than the expected stoichiometric value of 1.8% for complete reduction of Ga_2O_3 to Ga^+. Therefore, we conclude that a portion of gallium was ion-exchanged during sample preparation and calcination, as previously suggested.

The microbalance TA data for propanamines adsorbed on reduced Ga–MFI are depicted in Fig. 5. A comparison of reduced (Fig. 5) and unreduced (Fig. 3) samples results in several observations on the effect of reduction:

(a) The amount of the weakly bound 1-PA (given by Peaks A and B) decreases upon reduction, and a new shoulder (Peak G) on the DTA curve appears at about 530 K. Though it is perhaps difficult to see in the microbalance DTA curve, MS analysis (see below) confirms this new band;

(b) The amount of the weakly bound 2-PA represented

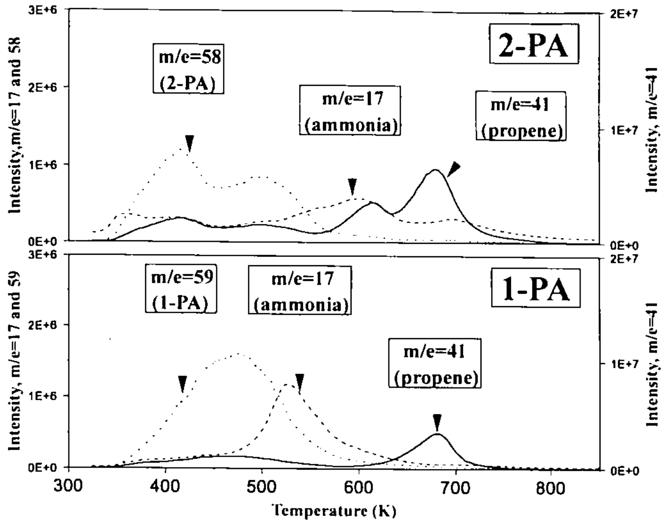

FIG. 6. Mass spectral analysis of the reactor effluent during thermal analysis of reduced Ga–MFI.

by Peak B on the DTA curve decreases sharply but a slight increase in the most weakly bound amine (Peak A) occurs;

(c) There is no clearly distinguishable plateau in the TA curves of either amine, but there is more 1-PA and less 2-PA in the plateau region for reduced samples;

(d) The DTA peaks C and E observed during TA of 1-PA on unreduced Ga–MFI are replaced by a single broad high-temperature peak denoted F in Fig. 5. Peak F is maximum at ~690 K, between the maxima of C and E in the unreduced sample;

(e) For 2-PA desorption, peak C is greatly diminished in Fig. 5 (reduced Ga–MFI). Meanwhile a new higher temperature peak appears in Fig. 5, whose maximum is located close to the maximum of peak F for 1-PA. An appreciable change in the shape of the DTA peaks for 2-PA on the reduced Ga–MFI catalyst should also be noted;

(f) An even larger weight offset at 823 K than for the unreduced samples is observed, corresponding to 17% of the calculated amount for formation of the 1 : 1 complex.

The overall process of desorption and decomposition of propanamines on reduced Ga–MFI is apparent in the MS analysis of the reactor effluent (Fig. 6). A comparison with analogous data for the unreduced Ga–MFI sample (Fig. 4) reveals, in accordance with the microbalance data, that the decomposition mode of propanamines changes radically as a result of the catalyst reduction. The most interesting phenomena are associated with ammonia desorption. For 1-PA decomposition on reduced Ga–MFI, ammonia (*m/e* = 17) desorbs almost completely at a temperature as low as 600 K (Fig. 6). The maximum of the ammonia desorption peak shifted more than 160 K, from 682 to 520 K, for unreduced and reduced Ga–MFI, respectively. Thus the formation of propene and ammonia during the TA of 1-PA does not occur simultaneously. However, different desorption features are found in the case of 2-PA. Although ammonia clearly begins to desorb prior to propene (*m/e* = 41, recall that at 550 K *m/e* = 41 represents fragmentation of propanamines), a large part of both products evolves in the same temperature range (550–800 K). The majority of the propene formed during decomposition of 2-PA on reduced Ga–MFI desorbs in exactly the same manner as the propene produced by decomposition of 1-PA.

In this investigation we applied mass spectrometry as an analytical method for product characterization analogous to previous work on propanamine decomposition (11–19). The complex desorption pattern observed for Ga–MFI, however, necessitated additional information on product composition by an independent method. For this purpose we analyzed by gas chromatography samples taken from the reactor effluent during the thermal analysis. Characteristic GC data are summarized in Table 1. As mentioned previously, it is evident that for H–MFI at temperatures below 600 K, unreacted propanamine is the sole product of TA. GC analysis also confirmed propene as the main product of 1-PA decomposition (ammonia cannot be detected by the flame ionization detector of the GC) on H–MFI at 703 K which is near the major DTA peak C. Side products consisted of ethene and butenes with only small amounts of saturated hydrocarbons. In contrast, a completely different composition of the desorption products was observed in the case of the reduced Ga–MFI. At a temperature of 523 K 1-PA was observed, as expected, as the main constituent of the reactor effluent, accounting for about 90% of the products. The remainder consisted primarily of propionitrile, whose concentration is much higher than that of the expected decomposition product propene. The changes in the product composition are even more pronounced for the sample that has been taken from the reactor effluent at a temperature of 673 K, at which the intensity of the "propene" (*m/e* = 41) goes through a maximum in Fig. 6. GC analysis revealed that in fact propene accounted for less than 43% of the reactor effluent and the propionitrile content was greater than the propene content. Besides propionitrile and propene, about 14% hydrocarbons ranging from ethene to hexenes were also present while again the amount of paraffins was very low.

The complexity of TA for propanamines on reduced Ga–MFI is further illustrated by the results for 2-PA decomposition. Table 1 shows 2-PA as the sole product desorbing at 403 K (corresponding to the low-temperature peak on the DTA and MS intensity curves). In the region of the first high-temperature DTA peak at 593 K (Fig. 5), the reactor effluent was found to consist mainly of propene, although isobutene and hexenes were present as

TABLE 1

GC Product Analysis of Reactor Effluent

	H–MFI		Ga–MFI reduced				
	1-Propanamine		1-Propanamine		2-Propanamine		
Temperature (K):	593	703	523	673	403	593	688
	% Product Based on GC Peak Area						
Methane							4.54
Ethene		2.20		1.77			2.79
Ethane		0.75		0.58			
Propene	0.50	92.34	2.73	42.89		88.82	24.69
Propane		0.67		0.78			
Isobutane		1.79		0.51			
butene-1 + isobutene		1.23		0.93		8.86	39.88
trans-Butene-2		1.02		0.85			1.88
cis-Butene-2				0.63			1.31
Pentene-1				0.53			
2-Methylbutene-1				0.83			
trans-Pentene				1.80			
cis-Pentene-2				0.92			
Hexene-1				0.59			
Other hexenes				2.94		2.32	
Benzene							3.40
Toluene							8.29
2-Propanamine					100.0		
1-Propanamine	99.50		90.09				
Acetonitrile			0.00		0.0		13.22
Propionitrile			7.18	43.46			

well. The composition of the product in the second high-temperature peak for 2-PA is represented by the sample at 688 K. Interestingly, the isobutene is now predominant. Other than methane, no paraffins could be detected. Moreover, acetonitrile, benzene, and toluene appear as significant products.

DISCUSSION

The primary goal of this investigation was to characterize changes in acidity due to the introduction of gallium into H–MFI zeolite using the method of propanamine decomposition developed by Gorte and co-workers (11–19). Since our experimental conditions deviate from those of the original method we have first verified the applicability of Gorte's method when performed in a conventional microbalance at atmospheric pressure. The data obtained for the H–MFI catalyst are consistent with the unimolecular decomposition of a propanammonium ion adsorbed on the zeolite protons which has been characterized in the literature as a Hofmann elimination (11–19),

$$C_3H_7NH_2 + HZ \rightleftarrows [C_3H_7NH_3]Z$$

$$[C_3H_7NH_3]Z \rightarrow C_3H_6 + NH_3 + HZ,$$

where Z is the zeolite framework.

While previous work on this topic has been based only on the fragmentation pattern of the desorbing propene, we have confirmed propene as the major product of 1-PA decomposition by means of GC. Even at a temperature of 703 K, which is after the maximum of the major DTA peak C, and even under the less favorable conditions (larger sample and deeper bed) of the flow reactor, the fraction of the hydrocarbons other than propene in the reactor effluent does not exceed 8%. No catalyst residue resulting from side reactions was observed during the microbalance experiments with either 1- or 2-PA. Thus, the interaction of the propanamine with the zeolitic protons plays a crucial role, and this modified TA method is suitable for counting the Brønsted acid sites provided that the catalyst is predominantly of the Brønsted type. It should be noted that the estimation of the number of Brønsted acid sites of an MFI zeolite is not based on the decomposition properties of propanamine. If one wants to count the proton acidic sites, it is necessary simply to determine the amount of propanamine that remains adsorbed in the "plateau" region of the TA curves. Our data confirm the literature findings that remarkably stable complexes with the zeolite protons are formed upon propanamine adsorption, and there are almost no weight changes in the "plateau" temperature interval, which is as wide as 70–80 K. It is important to note that readsorption, which is possible at the experimental conditions employed in our studies, can somewhat alter the desorption features of the decomposition products, but by no means will this physical phenomenon disturb the formation of the complexes themselves and therefore the level of the plateau. The unreacted propanamine desorbs separately before the "plateau" region of the TA curves.

The explanation of the desorption peaks for H–MFI at low temperatures is also an important point in our investigation. According to Gorte's data (16), 1.8 2-PA molecules per framework Al remain on an H–ZSM-5 zeolite at 400 K even after a prolonged evacuation. The authors of the original method "interpret this result as indicating that the molecules adsorbed in excess of the stoichiometric quantity are more weakly adsorbed and are not associated with acid sites" (13) and also note that if "internal silanols are responsible for these low-temperature features, proton transfer does not appear to occur" (16). We observed two distinct low-temperature desorption peaks (A and B) with both 1- and 2-PA (Figs. 1 and 3) eluting from H–MFI. All three major peaks (A, B, and C) for 2-PA are shifted to lower temperatures compared to 1-PA. Replacement of protons by Ga ions (Fig. 5) markedly affected the low-temperature desorption peaks. These results lead us to conclude that the low-temperature desorption states are indirectly associated with zeolite acid sites; we suggest the following:

$$xC_3H_7NH_2 + HZ \rightarrow \underset{\text{Peak C}}{C_3H_7NH_3Z} \cdot\cdot\cdot\cdot \underset{\text{Peak B}}{C_3H_7NH_2} \cdot\cdot\cdot\cdot \underset{\text{Peak A}}{(x-2)C_3H_7NH_2}.$$

It is well known that for ionic species, close-range nearest-neighbor interactions with solvent molecules are strong. These interactions depend on several factors such as charge, effective size, and the chemical nature of the ion. In accordance with the well-known chemistry of propanamines in solution, we assume that a second propanamine molecule is attached to each propanammonium ion formed in the zeolite, constituting a primary "solvation shell" whose breakup is characterized by DTA peak B. Proceeding outward, however, the influence of the ion must decline. As a result, the second "shell" whose breakup is characterized by peak A is less well defined and apparently can be eliminated by prolonged evacuation (13, 16). Another important factor in these relatively weak interactions are the limitations due to the zeolite structure and pore volume. While one propanamine molecule is clearly held in the first shell, as shown by both our microbalance data and Gorte's results, the second shell accounts for less than one propanamine per framework Al and there is evidently no place to accommodate a third propanamine molecule around the cation.

The most important finding in the present investigation, however, is related to the influence of the gallium cations on the desorption–decomposition features of propanamines. Our data indicate that the gallium ions which replace zeolitic protons strongly interact with the propanamine probe molecules (compare peak F in Fig. 5 with C in both Figs. 1 and 3). The nature of this interaction and the products of the decomposition are more complex than one might first assume considering only data from microbalance and mass spectral experiments. The analysis of the reactor effluent by GC showed that dehydrogenation reactions play an important role in propanamine decomposition on Ga-modified MFI zeolite.

The classic organic chemistry of amines is helpful in interpreting the results for Ga-modified zeolites obtained in this investigation. Besides accepting protons from Brønsted acids, amines can also add to Lewis acids by sharing the free electron pair. Good examples are the adducts between various amines and boron trifluoride (33). The ability to coordinate to metal ions is another well-known characteristic of amine groups. As in the case of ammonium complexes, the number of amine molecules which can be coordinated depends upon the electronic configuration of the metal. The Ag^+ ion coordinates two amine groups in a linear structure while Pd^{2+} and Pt^{2+} can coordinate four in square planar complexes, and other metals (Ni^{2+}, Co^{3+}) form octahedral complexes. The exposed cations of a zeolite are suitable for such interactions with amines, and so we suggest that the coordination of propanamines to zeolitic gallium cations is in large part responsible for peak E in Fig. 3 and F in Fig. 5. The different sizes of these peaks reflects the higher percentage of proton replacement by gallium in reduced (Fig. 5) versus unreduced (Fig. 3) Ga–MFI.

The TA–DTA results show that more than one 1-PA molecule is strongly held on reduced Ga–MFI at a temperature as high as 550 K, and that ammonia is the first product leaving the catalyst during the TA process. Therefore we propose the following idealized reactions for the interaction of 1-PA with reduced Ga–MFI catalyst:

$$2C_3H_7NH_2 + GaZ \rightarrow [(C_3H_7NH_2)_2Ga]Z$$

$$[(C_3H_7NH_2)_2Ga]Z \rightarrow NH_3 + [(C_3H_7)_2NH\,Ga]Z$$

$$[(C_3H_7)_2NHGa]Z \rightarrow C_3H_6 + CH_3CH_2C \equiv N + 2H_2 + GaZ.$$

Instead of a unimolecular decomposition of propanamines characteristic of the protonic zeolite, roughly two 1-PA molecules are coordinated to a gallium cation upon formation of a complex. As the temperature increases, the complex transforms with release of ammonia and a disubstituted amine is held on the cation. At higher temperatures, the decomposition features of the complex are strongly influenced by a dehydrogenation reaction leading to the formation of propionitrile and heavier products that show up as a residue. The final reaction shown above, although certainly a simplification of the actual chemistry, accounts for the observation (Table 1) that at 673 K propionitrile and propene are the primary products, formed in roughly equal amounts. The decomposition of 2-PA on reduced Ga–MFI is quite different. Local steric or other constraints on the complexes apparently do not allow the coordination of more than one 2-PA molecule to the cation. Consequently the condensation reaction giving rise to ammonia formation at 500–550 K (see Fig. 6) is suppressed. At near 600 K, the location of the first high-temperature peak in Figs. 5 and 6, a unimolecular complex apparently decomposes to primarily propene and NH_3. At higher temperatures, dehydrogenation, cracking and oligomerization reactions together lead to the complex product composition given in Table 1.

Finally, although most of the evidence for Lewis acid centers and their interactions with amines in this work is for the case of the reduced Ga–MFI catalyst, some results for the unreduced Ga-containing catalyst and the parent H–MFI suggest the presence of such sites in these samples as well. For example, the high-temperature DTA peaks D (Fig. 1) and E (Fig. 3) are certainly consistent with this interpretation, as are the $m/e = 17$ and $m/e = 41$ curves for 1-PA in Fig. 4. However, the high content of Brønsted centers in these samples makes it difficult to see so clearly the contributions of Lewis acid centers to the overall chemistry.

ACKNOWLEDGMENTS

The authors gratefully acknowledge the financial support of the Department of Energy (Grant #DE-FG05-92ER14291) and the Exxon Education Foundation.

REFERENCES

1. Chen, N. Y., *in* "Perspectives in Molecular Sieve Science," ACS Symposium Ser. 368 (W. H. Flank and T. E. Whyte, Jr., Eds.), p. 468. American Chemical Society, Washington, 1988.
2. Csicsery, S. M., *Pure Appl. Chem.* **58,** 841 (1986).
3. Chang, C. D., *in* "Perspectives in Molecular Sieve Science," ACS Symposium Ser. 368 (W. H. Flank and T. E. Whyte, Jr., Eds.), p. 596. American Chemical Society, Washington, 1988.
4. Harris, J. L., Krisko, N., and Wang, X. M., *Appl. Catal. A: General* **83,** 59 (1992).
5. Ward, J. W., *in* "Zeolite Chemistry and Catalysts," ACS Monograph 171 (J. A. Rabo, Ed.), p. 118. American Chemical Society, Washington, 1976.
6. Barthomeuf, D., *in* "Molecular Sieves II" (J. R. Katzer, Ed.), p. 453. American Chemical Society, Washington, 1977.
7. Dwyer, J., and O'Malley, P. Y., "Keynotes in Energy-Related Catalysis" (S. Kaliaguine, Ed.), Studies in Surface Science and Catalysis, Vol. 35, p. 5. Elsevier, Amsterdam/New York, 1988.
8. Rabo, J. A., and Gajda, G. J., *Catal. Rev.—Sci. Eng.* **31**(4), 385 (1989–90).
9. Jacobs, P. A., "Carboniogenic Activity of Zeolites." Elsevier, Amsterdam/New York, 1977.
10. Karge, H. G., *Z. Phys. Chem.* **122,** 103 (1980).
11. Grady, M. C., and Gorte, R. J., *J. Phys. Chem.* **89,** 1305 (1985).
12. Aronson, M. T., Gorte, R. J., and Farneth, W. E., *J. Catal.* **98,** 434 (1986).
13. Gricus Kofke, T. J., Gorte, R. J., and Farneth, W. E., *J. Catal.* **114,** 34 (1988).
14. Gricus Kofke, T. J., and Gorte, R. J., *J. Catal.* **115,** 233 (1989).
15. Gricus Kofke, T. J., Gorte, R. J., and Kokotailo, G. T., *Appl. Catal.* **54,** 177 (1989).
16. Gricus Kofke, T. J., Gorte, R. J., and Kokotailo, G. T., *J. Catal.* **116,** 252 (1989).
17. Parrillo, D. J., Adamo, A. T., Kokotailo, G. T., and Gorte, R. J., *Appl. Catal.* **67,** 107 (1990).
18. Biaglow, A. I., Adamo, A. T., Kokotailo, G. T., and Gorte, R. J., *J. Catal.* **131,** 252 (1991).
19. Parrillo, D. J., Pereira, C., Kokotailo, G. T., and Gorte, R. J., *J. Catal.* **138,** 377 (1992).
20. Zdrazil, M., *J. Catal.* **141,** 315 (1993).
21. Tittensor, J. G., Gorte, R. J., and Chapman, D. M., *J. Catal.* **138,** 714 (1992).
22. Parrillo, D. J., Dolenec, D., Gorte, R. J., and McCabe, R. W., *J. Catal.* **142,** 708 (1993).
23. Price, G. L., and Kanazirev, V., *J. Mol. Catal.* **66,** 115 (1991).
24. Park, Y. H., and Price, G. L., *Ind. Eng. Chem. Res.* **30,** 1700 (1991).
25. Vedrine, J. C., Auroux, A., Bolis, V., Dejaifve, P., Naccache, C., Wierzchowski, P., Van Hooff, J. H. C., Van Den Berg, J. P., and Wolthuizen, J., *J. Catal.* **59,** 248 (1979).
26. Nayak, V. C., and Choudhary, V. R., *Appl. Catal.* **4,** 333 (1982).
27. Joly, J. F., Ajot, H., Merlen, E., Raatz, F., and Alario, F., *Appl. Catal. A.* **79,** 249 (1991).
28. Kanazirev, V., Price, G. L., and Dooley, K. M., *J. Chem. Soc., Chem. Commun.* **9,** 712 (1990).
29. Price, G. L., Kanazirev, V., and Dooley, K. M., US Patent 5,449,579 (1992).
30. Kanazirev, V., Price, G. L., and Dooley, K. M., *in* "Zeolite Chemistry and Catalysis" (P. A. Jacobs *et al.*, Eds), p. 277. Elsevier, Amsterdam/New York, 1991.
31. Price, G. L. and Kanazirev, V., *J. Catal.* **126,** 267 (1990).
32. Kanazirev, V., Dimitrova, R., Price, G. L., Khodakov, A. Yu., Kustov, L. M., and Kazansky, V. B., *J. Mol. Catal.* **70,** 111 (1991).
33. Smith, J. W., *in* "The Chemistry of the Amino Group" (S. Patai, Ed.), p. 195. Interscience, New York, 1968.